Journal of Alloys and Compounds 615 (2014) 624–628

Contents lists available at ScienceDirect

Journal of Alloys and Compounds

journal homepage: www.elsevier.com/locate/jalcom

The spectroscopic properties of Dy^{3+} and Eu^{3+} co-doped $ZnWO_4$ phosphors

Yu Zhou, Jiayue Xu *, Zhijie Zhang *, Mingjiang You

Institute of Crystal Growth, School of Materials Science and Engineering, Shanghai Institute of Technology, 100 Haiquan Road, Shanghai 201418, PR China

ARTICLE INFO

Article history:
Received 12 May 2014
Received in revised form 7 July 2014
Accepted 8 July 2014
Available online 16 July 2014

Keywords:
$ZnWO_4$
Photoluminescence
Spectroscopic
Co-doped
W-LEDs

ABSTRACT

Dy^{3+} and Eu^{3+} co-doped $ZnWO_4$ phosphors with different doping concentrations were synthesized by a hydrothermal method. The as-prepared samples were characterized by X-ray diffraction (XRD), transmission electron microscopy (TEM) and photoluminescence (PL) spectra. The results showed that the doping concentrations of Eu^{3+} could affect the blue and yellow emission intensities of Dy^{3+}, and tunable emission color could be obtained by adjusting the doping concentrations of Eu^{3+}. Based on the excitation/emission spectra of Dy^{3+}/Eu^{3+} co-doped $ZnWO_4$ and the energy levels of Dy^{3+} and Eu^{3+}, the photoluminescence process in the Dy^{3+}/Eu^{3+} co-doped $ZnWO_4$ system was discussed in detail.

1. Introduction

Luminescent materials have attracted much attention in recent years for their potential application in LEDs [1–5]. It is known that there are three ways to develop white light: (i) the combination of UV-LED with red/green/blue (RGB) tri-color phosphors; (ii) the combination of blue LED with a yellow phosphor; and (iii) the combination of blue, green and red LEDs. Still more and more research groups [5–7] have made great efforts to develop single-phased phosphors for generating efficient warm white-light sources now. They hope that the phosphor has such advantages as better stability and reproducibility, no phase separation, and simpler preparation processes. The phosphor can be produced by co-doping a sensitizer and an activator in the same host matrix. Meanwhile, an effective resonance-type multipolar interaction has been verified [8–14].

In recent years, tungstates have been widely studied due to their good luminescent properties [15–21]. $ZnWO_4$ as a kind of significant luminescent materials, has also been investigated to generate white light [2,4]. However, the stability of $ZnWO_4$ after doped or co-doped by rare earth ion is not high enough for the requirements of practical application because it is a complicated system of photoluminescence. Though there are many papers on the luminescence property of $ZnWO_4$ [1,16–21], the detailed photoluminescence process of co-doped $ZnWO_4$ has seldom been studied.

It́s well-known that Dy^{3+} has two dominant emission bands, in which the yellow band corresponds to the ${}^4F_{9/2}$–${}^6H_{13/2}$ transition and the blue band corresponds to the ${}^4F_{9/2}$–${}^6H_{15/2}$ transition. In addition, adjusting the intensity ratio of the two hypersensitive transitions may generate white-light emitting [22,23]. This can be realized by co-doping Dy^{3+} and an appropriate rare earth ion into the host matrix.

Herein, the photoluminescence process of co-doped $ZnWO_4$ was studied, in which Dy^{3+} was selected as a sensitizer, and Eu^{3+} as an activator. The effect of doping concentrations of Eu^{3+}on the luminescent properties of Dy^{3+}/Eu^{3+} co-doped $ZnWO_4$ has also been investigated. A tunable emission color was realized by adjusting the doping concentrations of Eu^{3+}.

2. Experimental procedures

2.1. Synthesis

The experimental process of synthesizing $ZnWO_4$ powders was as follows: 2 mmol of $Zn(NO_3)_2{\cdot}6H_2O$ (A.R.) was dissolved in 10 mL of deionized water to obtain solution A. Meanwhile, 2 mmol of $Na_2WO_4{\cdot}2H_2O$ (A.R.) was dissolved in 10 mL of deionized water to obtain solution B. Then appropriate amount of $Dy(NO_3)_3$ and $Eu(NO_3)_3$ solution was slowly added to solution B under stirring. After that, solution A was added to the mixed solution to obtain a white suspension. The pH value of the suspension was adjusted to 8 by the addition of NaOH solution, then sealed in a Teflon-lined stainless steel autoclave and heated at 433 K for 16 h under autogenous pressure. The obtained solid product was washed thoroughly with deionized water and dried at 333 K. In this work, the atomic ratios of Dy^{3+}:Eu^{3+}:Zn^{2+} were 0.04:x:1 (x = 0.25%, 0.75%, 1.25%, 1.75%, 2.25%), respectively.

---

* Corresponding authors. Tel.: +86 21 6087 3581; fax: +86 21 6087 3439.
E-mail addresses: xujiayue@sit.edu.cn (J. Xu), zjzhang@sit.edu.cn (Z. Zhang).

http://dx.doi.org/10.1016/j.jallcom.2014.07.075

2.2. Characterization

The phase and composition of the as-prepared samples were measured by the powder X-ray diffraction (XRD) studies using a D/max-2200 PC type diffractometer (Rigaku Co. Ltd., Tokyo, Japan) with Cu Kα radiation (λ = 1.5418 Å). The morphologies of the products were obtained by transmission electron microscopy (FEI tecnai G2F30). The photoluminescence (PL) excitation and emission spectra of the samples was measured on an Edinburgh Instruments FLS920 spectrophotometer, using Xenon lamp as the light source.

3. Results and discussion

3.1. Crystal structure

The XRD patterns of the as-prepared $ZnWO_4$ samples with different doping concentrations (4% Dy^{3+}, y Eu^{3+}) were shown in Fig. 1. All the peaks in the patterns match well with the characteristic reflections of zinc tungstate (JCPDS No. 15-0774) when the doping concentration of Eu^{3+} was below 1.75%. No any other diffraction peaks belonging to the impurity phase were observed, which indicated that the products were pure phase. However, a few peaks (Fig. 1 ♦) of WO_3 appeared when the doping concentration of Eu^{3+} was above 1.75%.

3.2. Morphology

The morphologies and microstructures of the pure $ZnWO_4$ and Dy^{3+}/Eu^{3+} co-doped $ZnWO_4$ samples were investigated with TEM, as shown in Fig. 2. The TEM image in Fig. 2(A) showed that the pure $ZnWO_4$ exhibited nanorods structure and the nanorods were 40–60 nm in length. However, both nanorods and nanoparticles were observed for Dy^{3+}/Eu^{3+} co-doped $ZnWO_4$ sample (Fig. 2(B)), which indicated that doping Dy^{3+} and Eu^{3+} influence the growing interface and finally change the morphologies of $ZnWO_4$ according to the chemical bonding theory of single crystal growth [24–26]. Moreover, the HRTEM images showed clear lattice fringes of $d = 0.241$ nm for pure $ZnWO_4$ (Fig. 2(C)) and $d = 0.254$ nm for Dy^{3+}/ Eu^{3+} co-doped $ZnWO_4$ (Fig. 2(D)), which matched the d-spacing of the (0 2 1) plane of $ZnWO_4$.

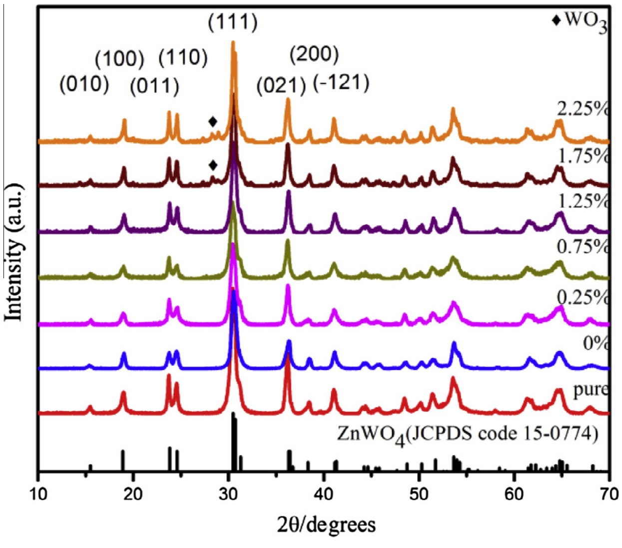

Fig. 1. Powder X-ray diffraction patterns for pure $ZnWO_4$ and 4% Dy^{3+}/y Eu^{3+} co-doped $ZnWO_4$ powders with different doping concentration.

3.3. Photoluminescence spectra

The excitation spectra of the 581 nm Dy^{3+} emission in Dy^{3+}/Eu^{3+} co-doped $ZnWO_4$ powders are shown in Fig. 3. It consisted of five sharp lines due to the transitions within the $4f^{11}$ shell of the Dy^{3+} and a broad band (230–340 nm) in the UV region. The broad band was due to the existence of WO_6 octahedral structures as the role of luminescence centers in the matrix. This optical transition involved in the luminescence of W–O groups was due to charge transfer between the O 2p orbitals and the empty d orbitals of the central W ion [27,28]. Moreover, there are five emission lines centered around wavelengths of 353 nm, 367 nm, 388 nm, 427 nm, 454 nm, which corresponded to the $^6H_{15/2} \rightarrow {}^6P_{7/2}$, $^6H_{15/2} \rightarrow {}^6P_{5/2}$, $^6H_{15/2} \rightarrow {}^4I_{13/2}$, $^6H_{15/2} \rightarrow {}^4G_{11/2}$, $^6H_{15/2} \rightarrow {}^4I_{15/2}$ transitions of Dy^{3+} ions, respectively. The emissions became weak gradually as the doping amount of Eu^{3+} ions increased (as shown in the inset of Fig. 3), which indicated that there was energy transfer between Dy^{3+} and Eu^{3+}, and the energy transferred from Dy^{3+} to Eu^{3+} due to their ionic electronegativity difference [29–31].

Fig. 4 showed the excitation spectra of the 615 nm Eu^{3+} emission in Dy^{3+}/Eu^{3+} co-doped $ZnWO_4$ powders. We can see clearly five emission lines (362 nm, 383 nm, 395 nm, 417 nm, 465 nm), which belonged to the transitions within the $4f^6$ shell of the Eu^{3+}. Moreover, the emissions became stronger gradually as the doping amount of Eu^{3+} ions increased, which indicated that the introduction of Eu^{3+} could enhance the fluorescence efficiency.

The emission spectra of Dy^{3+} single-doped and Eu^{3+}/Dy^{3+} co-doped $ZnWO_4$ under the same experimental conditions ($\lambda_{ex} = 294$ nm) were shown in Fig. 5(A) and (B), respectively. The intrinsic emissions of Dy^{3+} could be observed clearly in the emission spectrum of Dy^{3+} single-doped sample (Fig. 5(A)). There were two strong emissions centered at 489 and 581 nm and a weak emission at around 670 nm, which could be ascribed to the $^4F_{9/2} \rightarrow {}^6H_{15/2}$, $^4F_{9/2} \rightarrow {}^6H_{13/2}$, and $^4F_{9/2} \rightarrow {}^6H_{11/2}$ transitions of Dy^{3+}, respectively [22,32]. In the emission spectra of Eu^{3+}/Dy^{3+} co-doped sample (Fig. 5(B)), besides the intrinsic emissions of Dy^{3+}, the emissions of Eu^{3+} centered at 592, 598, 615,and 655 nm could be observed, which corresponded to the transitions from $^5D_0$ state to the ^7F_J (J = 0, 1, 2, 3) states, respectively [4,33,34].

The emission spectra of pure $ZnWO_4$ and Dy^{3+}/Eu^{3+} co-doped $ZnWO_4$ samples with different doping concentration were shown in Fig. 6. It could be seen that the emission spectra of pure $ZnWO_4$ consisted of a broad emission band at 400–700 nm. In the Eu^{3+} and Dy^{3+} co-doped system, blue (Dy^{3+}:$^4F_{9/2} \rightarrow {}^6H_{15/2}$), yellow ($Dy^{3+}$:$^4F_{9/2} \rightarrow {}^6H_{13/2}$), and red emission ($Eu^{3+}$:$^5D_0 \rightarrow {}^7F_2$) could be achieved. Moreover, with the increase of the doping concentration of Eu^{3+}, the red emission intensity increased and the yellow emission intensity became slightly weaker, while the effect on the blue emission intensity was not obvious. This indicated that it was possible to obtain white light by properly adjusting the doping concentrations of Eu^{3+} and Dy^{3+}.

3.4. Influence of Eu^{3+}concentration on the color coordinates

According to the Commission International de L'Eclairage (CIE) standard, the chromaticity coordinates of the $ZnWO_4$ samples were computed and were marked as points a, b, c, d, e, f and g in Fig. 7. As shown in Fig. 7, the emission color of pure $ZnWO_4$ (point a) was blue-green and the emission color of 4% Dy^{3+}-doped $ZnWO_4$ (point b) was yellow. After introducing proper amount of Eu^{3+}, the colorimetric performances of the phosphors were improved and the emission colors changed from yellow to orange with the increasing concentration of Eu^{3+}. Especially, the point e was located in the warm white light region when the doping concentration of Eu^{3+} was 1.25%. Therefore, the emission color can be easily tuned by appropriately adjusting the concentration of Eu^{3+} in a